Soluble Oligomers of the Intramembrane Serine Protease YqgP Are Catalytically Active in the Absence of Detergents

ARTICLE *in* BIOCHEMISTRY · NOVEMBER 2008

Impact Factor: 3.02 · DOI: 10.1021/bi800385r · Source: PubMed

5 AUTHORS, INCLUDING:

Lei Zhu
AMRI
10 PUBLICATIONS **219** CITATIONS
SEE PROFILE

Iban Ubarretxena-Belandia
Icahn School of Medicine at Mount Sinai
41 PUBLICATIONS **1,580** CITATIONS
SEE PROFILE

Published in final edited form as:
Biochemistry. 2008 November 18; 47(46): 11920–11929. doi:10.1021/bi800385r.

Soluble oligomers of the intramembrane serine protease YqgP are catalytically active in the absence of detergents

Xiaojun Lei[‡,§], **Kwangwook Ahn**[‡], **Lei Zhu**[‡], **Iban Ubarretxena-Belandia**[||], and **Yue-Ming Li**[‡,§,*]

‡ *Molecular Pharmacology and Chemistry Program, Memorial Sloan Kettering Cancer Center, New York, NY 10021*

§ *Department of Pharmacology, Joan Weill Graduate School of Medical Science of Cornell University, New York, NY 10021*

|| *Department of Structural and Chemical Biology, Mount Sinai School of Medicine, New York, NY 10029*

Abstract

Rhomboid, a polytopic membrane serine protease, represents a unique class of proteases that cleave substrates within the transmembrane domain. Elucidating the mechanism of this extraordinary catalysis comes with inherent challenges related to membrane-associated peptide hydrolysis. Here we established a system that allows expression and isolation of YqgP, a rhomboid homolog from *Bacillus Subtilis*, as a soluble protein. Intriguingly, soluble YqgP is able to specifically cleave a peptide substrate that contains the transmembrane domain of Spitz. Mutation of the catalytic dyad abolished protease activity, and substitution of another highly conserved residue Asn241 with Ala or Asp significantly reduced the catalytic efficiency of YqgP. We have identified the cleavage site that resides in the middle of the transmembrane domain of Spitz. Replacement of two residues that contribute the scissile bond by Ala did not eliminate cleavage, rather led to additional or alternative cleavages. Moreover, we have demonstrated that soluble YqgP exists as oligomers that are required for catalytic activity. These results suggest that soluble oligomers of MBP-YqgP form micelle-like structures that are able to retain the active conformation of the protease for catalysis. Therefore, this work not only provides a unique system to elucidate the reaction mechanism of rhomboid, but will also facilitate the characterization of other intramembrane proteases as well as non-protease membrane proteins.

Intramembrane proteases have emerged as a new class of membrane proteins, in which the catalytic residues of the protease reside within predicted transmembrane domains (1,2). Moreover, the scissile bond of substrates appears to be situated within a transmembrane domain as well. Three classes of intramembrane protease have been reported: 1) S2P-type metalloprotease that processes the transcription factor SREBP (the sterol regulatory element-binding protein) (3); 2) Presenilin/γ-secretase and signal peptide peptidase type aspartyl proteases that cleave multiple substrates with broad biological activities (4–6); 3) Rhomboid-type serine proteases that activate Spitz, a transmembrane ligand for the EGF receptor in *Drosophila* (7). Intramembrane proteases play an important role in many physiological processes, such as cellular differentiation, lipid metabolism, protein folding, and virus infection (8). Elucidating the catalytic mechanism of intramembrane proteases has been formidable

*To whom correspondence should be addressed: Molecular Pharmacology and Chemistry Program, Memorial Sloan Kettering Cancer Center, 1275 York Ave. New York, NY 10065; Tel 646-888-2193; Fax 646-422-0640; E-mail liy2@mskcc.org.

COMPLETING INTERESTS STATEMENT
authors declare that have no competing financial interests.

challenge that requires novel approaches to deal with membrane-associated enzymology, such as how to present an exogenous substrate to the protease and how to catalyze peptide hydrolysis in hydrophobic environments.

Rhomboid-1(Rho-1) was the first rhomboid discovered through a genetic screen in *Drosophila*, and loss of function of Rho-1 leads to the formation of a pointed head in the embryonic skeleton (9). Rho-1 and another membrane protein, Star, have been genetically linked with EGF receptor signaling in *Drosophila* through the release of a transmembrane ligand, Spitz (10). Rho-1, a polytopic membrane protein, has been shown to be a serine protease which converts inactive Spitz into its active form (7). Star acts as a chaperon protein that escorts the inactive Spitz precursor from the endoplasmic reticulum to the Golgi where Rho-1 cleaves Spitz to release the active form. Rhomboid is widely conserved in all organisms (11). Additional functions of rhomboid like proteins include quorum sensing in bacteria, host-invasion by parasites, mitochondrial remodeling and apoptosis in eukaryotic cells (12–16). The majority of examined rhomboids from mammalian to bacteria are able to process Spitz. Recently, rhomboids have been biochemically reconstituted using purified recombinant protein (17,18). These studies demonstrated that rhomboid is sufficient to exhibit protease activity, which is distinct from γ-secretase that is active as a macromolecular complex. Lately, crystal structures of rhomboids from *E. coli* and *Haemophilus influenzae* have been resolved (19–22). Structural studies have provided critical insights into the architecture of the catalytic center including the Ser-His dyad and the oxyanion hole for substrate binding and intramembrane proteolysis. Moreover, there is a gating mechanism that controls substrate entry into the hydrophobic active site. However, which protein domain functions as the gate remains a controversial matter. In addition, stable trimers or multimers of rhomboid have been observed and their function is unknown (18,20). The precise reaction mechanism of the rhomboid protease remains to be elucidated. Developing a system that enables determination of the kinetic parameters of rhomboid will facilitate the dissection of the reaction mechanism for substrate binding, catalysis and specificity of rhomboids, and will provide the molecular basis for structural and functional studies as well as for designing mechanism-based inhibitors.

In the present study, we overexpressed and purified full-length YqgP, a rhomboid homolog from *Bacillus Subtilis*, fused with maltose binding protein (MBP) at the N-terminus. Strikingly, MBP-YqgP can be isolated as a soluble protein in the absence of any detergent. More importantly, soluble MBP-YqgP is able to cleave a substrate that contains the transmembrane domain of Spitz without reconstitution into a lipid or detergent system. Biochemical and biophysical studies suggest that MBP-YqgP oligomerizes into complexes that mimic the micelle-like environment and permit catalysis. Moreover, mutagenic, kinetic and inhibitor analyses have shown that the activity of recombinant MBP-YqgP exhibits the characteristics of rhomboid as seen in cellular studies and YqgP isolated from membrane fractions.

EXPERIMENTAL PROCEDURES

Cell lines and Reagents

Genomic DNA of *Bacillus Subtilis* and COS-1 were obtained from American Type Culture Collection (ATCC). *DH5α* and *BL21 (DE3)* strains were purchased from Invitrogen. Plasmids pcDNA3.1-Rhomboid-1, pcDNA3.1-Star, pcDNA3.1-RHBDL2, and pcDNA3.1-Spitz were kindly provided by Dr. Matthew Freeman of the MRC Laboratory of Molecular Biology, UK. The following antibodies were used in the study: mouse monoclonal antibodies 9E10 against the Myc epitope (Monoclonal antibody facility, Memorial Sloan Kettering Cancer Center, New York, NY), and mouse monoclonal antibodies against β-tubulin, HA, and VSV-G (Roche Diagnostics, Indianapolis, IN).

Plasmid Constructs

All constructs used for mammalian transfection were built in pCDNA3.1. A Myc tag was introduced into pCDNA3.1-Spitz between residues 80 and 81. Three rhomboids (Rho-1, RHBDL2 and YqgP) were fused with the VSV-G tag (peptide sequence: YTDIEMNRLGK) on the C-terminus (Figure 1B). The Plasmid pIAD16-YqgP was generated by inserting YqgP gene into the bacterial expression vector pIAD16 (23) using the *Nde I* and *Hind III* restriction sites with MBP tag at the N-terminus. QuikChange Site-Directed Mutagenesis Kit (Stratagene) was used to generate mutated constructs.

Peptide Synthesis

All peptides in this study were synthesized using standard Fmoc solid phase chemistry on a peptide synthesizer (Protein Technologies, Inc.). The same method was used to incorporate Fmoc protected (MCA)-K (N-ε-[(7-methoxycoumarin-4-yl)-acetyl]-L-lysine), a fluorescent amino acid, into substrate peptides. All peptides were purified by high-pressure liquid chromatography (HPLC) on a reverse-phase C18 column. The identity of the peptides was verified by LC-MS/MS (Agilent Technologies).

Cell culture, transfection and lysate preparation

COS-1 cells were grown in high glucose Dulbecco's modified Eagle's medium (DME) supplemented with 10% fetal bovine serum, 100 U/ml penicillin, 100 μg/ml streptomycin. Transfection was conducted in 6-well plates with FuGENE 6 transfection reagent (Roche Diagnostics) according to the manufacturer's protocol. The cells were incubated at 37°C for 48h, and then washed with cold PBS three times before being scraped off the plate. Cell pellets were lysed with RIPA buffer (Tris-HCl 50 mM, pH 7.4, NP-40 1%, Na-deoxycholate 0.25%, NaCl 150 mM, SDS 0.1%), EDTA 1 mM, and 2mM DTT, and Protease inhibitor Cocktail (Roche Diagnostics).

Overexpression and purification of YqgP

The plasmid pIAD16-YqgP was transformed into the BL21(DE3) cells for protein expression. When bacteria cells reached 0.8 at OD600, IPTG in a final concentration of 0.1 mM was added to induce the target protein expression at 20°C for 5 hr. Cell pellets that were resuspended in buffer A (20mM Tris, 200 mM NaCl, pH 7.5) were broken by a French press (Spectronic Instruments, Rochester, NY). Cell lysates were centrifuged at 10,000g for 45 min. The supernatants then were centrifuged at 100,000g for 60 min. The ensuing supernatant was applied to the amylose column and eluted with a gradient of buffer A containing 10 mM maltose. The eluted proteins were analyzed by SDS-PAGE and pooled for studies. In addition, we have solubilized and purified the YqgP protein from membrane fractions by following the same procedure as described (18). The identity of YqgP proteins was confirmed by trypsin digestion and LC-MS/MS analysis.

In vitro cleavage assay and cleavage site mapping

The recombinant MBP-YqgP (15 μg) was incubated with 2μM of peptide substrate in 100 μl of assay buffer (50 mM PIPES, pH 7.0, 4mM dithiothreitol) at 37°C for 3 hours. The reaction was stopped by adding 5μl 5% TFA in water and centrifuged at 10,000g for 10 min. Internal fluorescent standard MCA was spiked in each reaction for calculation and normalization of the cleaved product. The supernatant of reaction mixture (90 μL) was analyzed by reverse-phase HPLC equipped with a fluorescent detector on a ZORBAX 300 SB-C18 4.6X150 mm column (Agilent Technology). Fluorescence signal was monitored with excitation 340 nm and emission 405 nm. All peaks were integrated and normalized with the internal standard for product quantification.

Electron Microscopy

Negatively stained specimens were prepared by applying 2uL (0.2mg/ml) of MBP-YqgP solution on glow discharged carbon-coated cooper grids followed by washing and blotting with 1% uranyl acetate. Samples were examined in a JEM-1230 electron microscope (JEOL, Tokyo Japan) at an accelerating voltage of 80keV and images were recorded on a 1kx1k CCD camera (Erlangshen, Gatan Inc, Pleasanton CA).

Lipid analysis of purified MBP-YqgP

Lipid analysis was performed with a procedure as described (24). Briefly, purified MBP-YqgP (10ul 1mg/ml) was mixed with 40ul of chloroform/methanol (1:2, v/v) and spotted onto a TLC plate (silica gel 60 F254, Merck). Various amount of total lipid extract from *E. Coli* (Avanti Polar Lipids) was spotted as a positive control. After sample spots completely dry, the TLC plate is resolved in chloroform/methanol/25% aqueous ammonia (Volume ratio as 65:25:5). The lipid is visualized by spraying the dried plate in 0.1% of 8-anilino-1naphthalene sulfonic acid (Sigma) under UV light.

Reconstitution of YqgP into proteoliposome

Medium, 100-nm unilamellar vesicles were made from mixtures of lipids using extrusion. 400 μL (3.2mg of total lipid) of freshly prepared batch of MUV(medium unilamellar vesicle) was mixed with 25.6 μL of 10 % CHAPS - lipid: detergent ratio = 1:0.8 (w/w) and end-over-end rotation at 4 °C for 1 hr. MBP-YqgP (0.514 mg/mL) was added to liposome-detergent mixture at 1:100 of protein: lipid ratio (w/w) and end-over-end incubation at 4 °C for 2 hr. Detergent removal was initiated by incubation with SM-2 bead (200–300 mg/each cycle) at 4°C for 1 hr and completed by dialysis with resuspension buffer (total 4L) for 6 hr at 4°C. The dialysates was treated with Thrombin at 16°C for 3 hr to remove MBP tag. The YqgP proteoliposomes were incubated with substrate and the product was analyzed by HPLC as described above.

RESULTS

High expression levels of rhomboid can process Spitz in the absence of Star in cells

Three rhomboid proteins, Rho-1 from *Drosophila*, RHBDL2 from human, and YqgP from *Bacillus Subtilis*, all of which show conservation of the catalytic dyad (Ser-His) and a highly conserved residue Asn, were selected and tagged to determine their activities (Figure 1A and B). Both rhomboid and Spitz were co-transfected with or without Star, the chaperon which is required to export Spitz to the Golgi complex where rhomboid cleaves Spitz. YqgP alone is capable of cleaving Spitz (Figure1C, lane 3, upper panel), whereas RHBDL2 and Rho-1 appear to require the presence of Star (Figure 1C lane 4, 5 and lane 7, 8, upper panel). However, Star does enhance the processing of Spitz by YqgP (Figure 1C, lane 3 vs 6, upper panel). Upon further examination of the expression of YqgP, RHBDL2 and Rho-1, we found that the expression level of YqgP is much higher than the other two proteins (Figure 1C lower panel). We reasoned that overexpression of rhomboid overcomes the requirement of Star. To test whether Spitz cleavage is dependent on the amounts of expressed rhomboid, we elevated the expression of rhomboid through transfection with increasing DNA input. As expected, the cleaved Spitz product was detected in the absence of Star when 1 μg plasmid of Rho-1 or RHBDL2 was transfected (Figure 1D). Therefore, these studies suggest that Rhomboids are capable of cleaving Spitz in the absence of Star if Rhomboid expression levels are high enough and YqgP is a good candidate for the reconstitution of proteolytic activity.

Soluble recombinant YqgP is catalytic active

We attempted to express YqgP as a soluble protein by fusing it to the maltose binding protein (MBP). The MBP tag without signal sequence that directs target protein into membranes was

fused with the YqgP protein at the N-terminus in a pIAD16 plasmid (23). The fusion protein was expressed in *E. coli* and isolated from the 100,000 g supernatants using an amylose column in the absence of detergent. The purified protein was analyzed by SDS-PAGE (Figure 2A, lane 1). A major protein band with MW of 100kDa that corresponds to the fused protein of MBP-YqgP was observed (Figure2A). Moreover, tandem mass analysis of in-gel digested band confirmed its identity as MBP-YqgP protein (data not shown). Two minor bands migrate with molecular masses of 58 kDa and 44 kDa, which were identified by LC-MS/MS as MBP plus partial N-terminal fragment of YqgP that contains no key residue of Asn, Ser, or His, and MBP, respectively. Employing the same strategy, we were able to overexpress and purify four mutant YqgP proteins, N241A, N241D, S288A and H339A, with the same purity (Figure 2A, lanes 2–5). These MBP-YqgP proteins were isolated in high yield with approximately 2 mg from one liter of bacterial culture. To confirm that bacterial lipids were not co-purified in our protein samples, we performed lipid analyses of purified MBP-YqgP (Figure 2B). The detection limit of the assay was 0.2 μg of lipid and even when 10μg of purified protein were assayed no lipid traces were detected, indicating the absence of significant amounts of lipid in our preparation.

Since YqgP cleaves Spitz to release the ligand domain for EGFR signaling, we chemically synthesized a peptide that contains the transmembrane domain of Spitz and a MCA((7-methoxycoumarin-4-yl)acetyl) fluorescent tag that allows for the detection and quantification of the cleaved products with high sensitivity (Figure 2C). After the recombinant soluble MBP-YqgP was incubated with the peptide substrate $Spitz_{TMD}$, the reaction mixture was analyzed by HPLC equipped with a fluorescent detector. In addition to the substrate peak (S) eluting at 20 min, a major new peak (P) at 15.5 min was detected from the reaction mixture of MBP-YqgP and Spitz peptide (Figure 2D, WT, blue line). In order to rule out that this cleavage product peak (P) was produced by an unknown protease which co-purified with rhomboid, the Spitz peptide was incubated with a catalytically-dead mutant in which the active site nucleophile Serine residue is substituted by Ala (S288A). No peak P was detected in the S288A reaction (Figure 2D, S288A, red line). Moreover, the H339A mutant in which the active site His residue is replaced by Ala led to no product formation (data not shown). These studies confirm that the cleaved product (peak P) of Spitz peptide is derived from MBP-YqgP activity

After validating this *in vitro* assay, we determined the inhibitor profiles of YqgP using established serine protease inhibitors: 3,4-dichloroisocoumarin (DCI), tosyl-L-phenylalanine chloromethyl ketone (TPCK), tosyl-L-lysine chloromethyl ketone (TLCK), diisopropylfluorophosphate(DFP), and phenylmethylsulfonyl fluoride (PMSF). DCI at a concentration of 400 μM blocks 35% of protease activity; whereas other tested inhibitors have no considerable effect (Figure 2E). Other studies suggest that DCI at 100–400 μM completely inhibits YqgP activity (17, 18). We reasoned that slow entrance of DCI to the active site in the presence of substrate caused a moderate inhibition. To test this notion, we have preincubated DCI with MBP-YqgP at 400 μM for 60 min and then added substrate to test remaining protease activity. We found that DCI at 400 μM was capable of totally abolishing YqgP activity (data not shown).

Next, we examined the effect of detergents on the MBP-YqgP protease activity (Figure 2F). CHAPS at 0.1% and 0.25% stimulated MBP-YqgP activity 2.1 and 1.8-fold, respectively. However, higher concentrations (0.5 and 1.0 %) significantly suppressed the protease activity (>85% inhibition). CHAPSO has a similar tendency as CHAPS except for that it reduced the activity at 0.25%. However, the presence of DDM ranging from 0.01 to 1% leads to a similar reduction in MBP-YqgP activity (40–45%). MBP-YqgP shows no activity in the presence of Triton X100 (0.1–1%) (Data not shown). It appears that detergents potentiate the proteolytic activity when their concentration is considerably lower than the critical micelle concentration (CMC), and they attenuated or abolished the activity when the concentration of detergents is close to or at the CMC. Subsequently, we inserted YqgP into liposomes and determined its

activity. The YqgP-proteoliposomes manifested 3.3-fold higher activity than soluble YqgP (Figure 2F). In other words, the specific activity of YqgP in the absence of detergent or membranes is 30% of YqgP when it is engaged in the lipids.

We next mapped the cleavage site through tandem MS analysis. The peak P was collected from HPLC and analyzed with Agilent LC-MS/MS. A single peak with m/z =655 was detected (Figure 3A). This peak matches the mass of a peptide: MCA-KEKASIASGAM with double charges (z= 2, measured mass = 1308, calculated mass =1309). A tandem mass analysis (MS/MS) of 655 mass peak detected a series of mass fragments, 602.2, 673.2, 760.2, 873.3, 944.2, 1031.2, 1088.3 and 1159.3, which perfectly matched to b_3 to b_{10} ions of assigned peptide sequence, respectively (Figure 3B). This result clearly indicated that MBP-YqgP specifically cleaves the peptide bond between Met and Cys on Spitz. To further determine the role of the Met and Cys residues in substrate recognition, the two residues were separately replaced by Ala in Spitz resulting in two mutants: M145A and C146A. Each mutation was co-transfected with YqgP in COS-1 cells to assess their effects on Spitz cleavage by YqgP. Both substrate mutants (M145A and C146A) can still be effectively processed by YqgP-expressing cells, but not by the empty vector-expressing cells (Figure 3C). Subsequently, we synthesized peptide substrates with the M145A or C146A mutation and determined the cleavage site. HPLC analysis showed that both peptide substrates can be cleaved by MBP-YqgP as well with the same rate (Data not shown). However, LC-MS analyses have revealed an extra species with a molecular mass of 1450 (m/z = 726, z=2) that co-migrated with the 1308 product in HPLC for the C146A substrate (Figure 3D). The M145A mutation caused a shift in the cleavage site towards C-terminus by two and three residues. There are two cleaved products that are 1420 (m/z = 711, z= 2) and 1534 (m/z = 768, z= 2) for the M145A substrate (Figure 3D). The identity of these species was confirmed by LC-MS/MS. Moreover, these products were not detected when each substrate was incubated with the S288A mutation (data not shown).

Finally, we compared the reactivity and specificity of the soluble form of MBP-YqgP with the membrane-associated one. YqgP-His6 was expressed in E. coli and solubilized with 1% DDM from bacterial membranes. YqgP was purified (Figure 3E), and then incubated with the $Spitz_{TMD}$ substrate and the protease activity was analyzed as above. A product peak (P) migrated at the same position as observed with soluble MBP-YqgP (data not shown, see Figure 2D). This peak was collected and analyzed by LC-MS/MS. Again, it appeared as a single peak with m/z=665 (data not shown). Tandem mass spectra confirmed that the exact same product was generated by both the membrane associated and the soluble form YqgP. We further assessed the protease activity of soluble and membrane associated YqgP (Figure 3F). If we normalized the protease activity of MBP-YqgP in the absence of detergent as 100%, MBP-YqgP and YqgP in the presence of DDM represent 53% and 150% of activity, respectively. These studies indicate that soluble MBP-YqgP exhibits similar activity and the same specificity as the membrane form of YqgP.

Mutations of conserved Asn241 significantly reduce catalytic efficiency of MBP-YqgP

In addition to Ser and His residues, classical serine proteases contain an Asp residue that forms a triad to enhance the nucleophilicity of Ser by orienting His, whereas rhomboids possess a conserved Asn residue instead. In order to investigate the effect of Asn on catalysis, this residue was substituted with different residues. First, we replaced Asn by Ala (N241A) and determined the kinetic parameters of YqgP proteins. Values of Km and Vmax are 0.70 ± 0.14 μM and 4.05 ± 0.18 pmol min^{-1} μg^{-1} for WT, and 0.58 ± 0.18 and 0.61 ± 0.074 for the N241A, respectively (Figure 4). These results suggest that replacement of Asn241 by Ala leaves the Km unchanged, but substantially reduces its Vmax to 15% of WT value. In other word, the N241A mutation does not affect the interaction between substrate and protease, but rather diminishes the catalytic power of the His-Ser pair. Next, we mutated Asn to Asp (N241D) to check whether

Asp could restore or enhance the catalytic activity of the His-Ser dyad. The N241D mutant exhibits the same Km (0.64 ± 0.25 μM) as WT (Figure 4). However, Vmax value (0.95 ± 0.06 pmol min^{-1} μg^{-1}) is 23% of WT and 155 % of the N241A.

Soluble MBP-YqgP proteins assemble into oligomers for catalysis

An intriguing question is how the multiple-pass transmembrane protein MBP-YqgP stays soluble and exhibits catalytic activity in the absence of detergent. Since amphiphilic molecules in aqueous solutions spontaneously form micelles or vesicles, we hypothesize that MBP-YqgP, which consists of the hydrophilic soluble domain MBP and a hydrophobic membrane protein YqgP, oligomerizes to form micelle-like structures - in which MBP faces bulk water while YqgP remains in a hydrophobic environment (Figure 5A). In other words, oligomerization of YqgP leads to the formation of high molecular weight complexes that are required for its proteolytic activity. To test this hypothesis, we initially separated the complexes by gel-filtration chromatography and determined the active fraction by using our *in vitro* assay (Figure 5B). There are two major peaks detected by absorbance at 280 nM (Figure 5B, red dotted line), high (H) and low (L) molecular weight peaks that migrate at approximately 2000 and 140 kDa, respectively. The H peak exhibited the greatest protease activity and the L fraction had no detectable activity. In addition, fractions with molecular masses more than 300 kDa displayed moderate protease activity. These studies indicate that MBP-YqgP needs to form at least a trimer for catalytic activity and the majority of MBP-YqgP assemble into mega-molecular complexes. Next, we imaged the MBP-YqgP aggregates by negative-stain electron microscopy (EM). The field view displayed in Figure 5C shows MBP-YqgP complexes that are large and heterogeneous in size. It should be noted that MBP (44 kDa) has dimensions of ~30×40×65Å and YqgP, with a MW of 56 kDa should have, to a good approximation, comparable dimensions. Thus the average size (>250Å in any dimension) of the imaged complexes suggests that these complexes correspond to multimeric aggregates of MBP-YqgP. Remarkably the addition of 0.1 % CHAPS that augments protease activity to the sample did not have an effect on aggregate size (not shown). Next, we imaged the highly active 2000KDa MBP-YqgP fraction after size exclusion chromatography. The eluted complexes are very homogeneous in size with average dimensions of 350×250Å (measured from 10 individual particles) (Figure 5D). Taken together, these results suggest that the majority of MBP-YqgP aggregates into large stable multimeric structures that preserve YqgP activity. It is known that aqueous solutions generally quench fluorescence by orienting around the excited state dipoles and the partition of fluorescent molecules into detergent micelles or the membrane bilayer reduces quenching (28). We argued that if the interior of the MBP-YqgP oligomers is hydrophobic relative to bulk water, the partition of a fluorescent molecule into the micelle-like structure should reduce water-quenching. To this end, we examined the effect of MBP-YqgP oligomers on the fluorescence intensity of our synthetic substrate. To eliminate artifacts due to enzymatic activity, we used the catalytically dead MBP-YqgP-S288A mutant. MBP-YqgP-S288A or MBP was incubated with the substrate and the fluorescence intensity was monitored. Net fluorescence intensity change was calculated by subtracting the fluorescence intensity of fluorogenic substrate in the presence of MBP from that observed in the presence of MBP-YqgP-S288A. In this experiment MBP serves as a background control for non-specific MBP/substrate interaction. The inset scheme shows the fluorescent signal of MBP, substrate, or enzyme alone at different time points. The difference in net fluorescent change between MBP-YqgP and MBP is attributed to the partition of substrate into rhomboid oligomers(Figure 5E). These studies provide additional lines of evidence suggesting that the MBP-YqgP oligomers form micelle-like catalytically competent structures.

DISCUSSION

Intramembrane proteases are polytopic membrane proteins that cleave substrates within the transmembrane domain, an apparently hydrophobic environment. Rhomboid, an intramembrane serine protease, plays a pivotal role in cellular signaling. The present work developed an expression system that allows production of highly purified MBP-YqgP as a soluble protein in the absence of detergents. Surprisingly, soluble MBP-YqgP is capable of cleaving a peptide substrate derived from Spitz protein. Moreover, this system allows kinetic characterization of YqgP and elucidation of the reaction mechanism in detail. Finally, We have demonstrated that soluble MBP-YqgP forms oligomers or mega-molecular multimers, suggesting these functional aggregates may mimic the micelle-like environments required for peptide hydrolysis.

Biochemical reconstitution of bacteria S2P (RseP or YaeL) and rhomboids (YqgP from *B. Subtilis*, and GlpG from *E. col*i) has been reported (17,18,25). All recombinant proteins were solubilized from bacteria membrane and purified for reconstitution. *In vitro* protease activity was detected either by western blotting (25) or autoradiography (18). Our system expresses purified MBP-YqgP as a soluble protein without the requirement of detergent. Soluble MBP-YqgP exhibits protease activity for hydrolysis of the Spitz peptide substrate. Importantly, this activity is abolished by mutation of the key catalytic residues Ser (S288A) and His (H339A) and inhibited by DCI, which is corroborated with previous reconstitution studies using membrane solubilized YqgP (17,18). Taken together, these studies have established that the cleavage activity is attributed to the recombinant YqgP, rather than contaminated soluble proteases co-purified with the target protein. The next critical question is how active are the soluble YqgP aggregates compared with YqgP in the solubilized states or membranes. We have demonstrated that soluble MBP-YqgP displayed comparable protease activity (70%) as membrane solubilized YqgP. In addition, although there is no kinetic or enzymatic rate data from other reconstitution systems allowing for a direct comparison to soluble YqgP, the fraction (40–80%) of substrate conversion to product by the soluble YqgP is similar to that in the solubilized YqgP (18) after normalizing for the enzyme concentration and incubation times. Low turnover of solubilized intramembrane proteases has been observed in rhomboids (18) and γ-secretase (Vmax = 11.8 pm/min) (26). These studies suggest the soluble YqgP exhibits reasonable protease activity in the absence of detergent and membranes

LC-tandem MS analysis mapped the cleavage site between Met and Cys, which is close to the estimated processing site from cellular studies (7). This work has illustrated that the transmembrane domain of Spitz is sufficient to serve as a substrate for MBP-YqgP, which is consistent with cellular and biochemical studies (18,27). Importantly, we have demonstrated that soluble MBP-YqgP possesses the same specificity as membrane associated YqgP. Furthermore, replacement of Met145 or Cys146 by Ala in Spitz led to the generation of additional or alternative cleavage sites. If these peptides are considered to form α-helical structure, which is a favorable conformation that the transmembrane domains tend to fold (28), these cleavage sites would locate in different faces of the helix (Figure 6). The C146A allows protease to access scissile bonds from opposite directions, whereas the M145A results in generation of two novel cleavage sites on Spitz substrate. How these mutations affect the conformation of substrates and lead to the alternation of interaction between substrate and protease require more biophysical and structural studies. These findings support the notion that the major determinant of specificity for rhomboid is the conformation of substrate, rather than primary sequence (27). It has been reported that GlpG cleaves both Ala-Ser and Gly-Ala bonds in a hybrid substrate in which the first seven residues of the amyloid precursor protein (APP) transmembrane domain were replaced by the corresponding Spitz peptide (ASIASGA) (17, 29) that is recognized by rhomboid (27). Whether distinct cleavage sites result from different

substrates and/or different rhomboids remains to be investigated. Multiple cleavage sites have been observed in γ-secretase for APP and Notch processing (30).

Cellular mutagenesis studies suggested that rhomboid could contain an Asn-His-Ser triad for catalysis (7). However, structural studies have demonstrated that Asn is not proximate to the Ser-His pair for hydrogen bonding to stabilize the His residue. Therefore, rhomboid belongs to a class of dyad serine hydrolases (19,20) in which the His-Ser ion pair is capable of performing effective catalysis. The side chain of Asn is likely involved in the formation of oxyanion hole to enhance catalysis (31). However, mutation of Asn residue did not affect *in vitro* YqgP activity (18), which is in contrast to cellular studies in which Asn mutations considerably reduced and blocked rhomboid protease activity (32). N241A or N241D mutations in this study resulted in a reduction of catalytic efficiency of MBP-YqgP 6-and 4-fold, respectively. If Asn is one of the catalytic residues, it was expected that the effect on rate by these mutations would be much more dramatic ($>10^3$ fold), such as trypsin (33) and subtilisin (34) in which catalytic Asp was replaced by Ala. In this regards, MBP-YqgP is more closely related to the outer membrane phospholipase (OMPLA) that is an integral membrane enzyme with conserved Asn-His-Ser residues(35). Replacement of Asn by Ala and Asp in OMPLA led to 20- and 2-fold decrease in activity, respectively (36). We have also demonstrated that these mutations have no effect on the interaction of substrate-protease, but affect the catalytic power. Taken together, these findings indicate that Asn does not directly contribute to catalysis, but plays a critical role in rhomboid activity, which is corroborated by previous conclusion from structural and cellular studies (19–21,29,32).

Our study has shown that soluble MBP-YqgP proteins form oligomers or multimers for catalysis. Stable trimers or multimers of rhomboid have been observed in other studies (18, 20). In addition, the formation of oligomers has been observed in other intramembrane proteases, such as γ-secretase (37,38) and SPP (39,40). We demonstrated that γ-secretase activity is associated with the PS1-containing macromolecular complex with an apparent molecular mass of ~2000 kD(41). *Gu* et al. (42) detected two γ-secretase macromolecular complexes with molecular masses of ~440 kDa and 670 kDa, respectively. The higher molecular mass complex may be oligomers of the γ-secretase complex. It is apparent that intramembrane proteases commonly form oligomers, at least in solubilized states, and the oligomers' function in proteolysis may be related to the extraordinary catalysis of these intramembrane proteases. Their roles under physiological condition remain to be investigated.

MBP has been proven to be a valuable tag to assist soluble protein expression and isolation (43). However, when MBP was utilized for the expression of membrane proteins with multiple transmembrane domains, solubilization and refolding were needed to obtain functional proteins (43–45). The present experimental system allows us to directly generate soluble protein without the requirement of detergents. More importantly, this soluble fusion membrane protein (MBP-YqgP) is functionally active in the absence of detergent. Therefore, in addition to providing a practical system for studying rhomboid enzymology, this system may also be applicable for other intramembrane proteases. Whether this system can be utilized to express and isolate certain membrane proteins in soluble form and investigate their structure and function remains to be tested. Furthermore, purified MBP-YqgP can be utilized for reconstitution studies with detergents and/or lipids.

In summary, we successfully overexpressed MBP-YqgP in a soluble form without detergents, and reconstituted Rhomboid cleavage in an *in vitro* system. This assay could be an important tool for characterization of Rhomboid proteases. Furthermore, our system could be used as an experimental system to characterize other intramembrane proteases as well as other membrane proteins.

Acknowledgements

This work is supported by NIH grant AG026660 (YML), the Alzheimer's Association (Zenith Fellows Award to YML) and the American Health Assistance Foundation (YML). IU-B was supported by National Science Foundation Grant MCB-0546087.

We thank Lisa Placanica and Christopher C. Shelton for critical readings of the manuscripts; Dr. Christopher T Walsh for the pIAD16 plasmid. Dr. Matthew Freeman for Rhomboid and Spitz-1 constructs. We also thank the New York Structural Biology Center for electron microscope access.

Abbreviations and Textual Footnotes

CHAPS
3-[(3-Cholamidopropyl)dimethylammonio]-1-propanesulfonate

CHAPSO
3-([3-Cholamidopropyl]dimethylammonio)-2-hydroxy-1-propanesulfonate

DCI
3,4-dichloroisocoumarin

DDM
dodecyl-b-D-maltoside

DFP
Di-isopropylfluorophosphate

MBP
maltose binding protein

MCA
N-ε-[(7-methoxycoumarin-4-yl)-acetyl]

PMSF
Phenyl-Methyl-Sulfonyl Fluoride

S2P
site-2 protease

TLCK
Tosyl Lysyl Chloromethyl Ketone

TMD
transmembrane domain

TPCK
Tosyl phenylalanyl chloromethyl ketone

References

1. Brown MS, Ye J, Rawson RB, Goldstein JL. Regulated intramembrane proteolysis: a control mechanism conserved from bacteria to humans. Cell 2000;100:391–398. [PubMed: 10693756]
2. Wolfe MS, Kopan R. Intramembrane proteolysis: theme and variations. Science 2004;305:1119–1123. [PubMed: 15326347]
3. Rawson RB, Zelenski NG, Nijhawan D, Ye J, Sakai J, Hasan MT, Chang TY, Brown MS, Goldstein JL. Complementation cloning of S2P, a gene encoding a putative metalloprotease required for intramembrane cleavage of SREBPs. Mol Cell 1997;1:47–57. [PubMed: 9659902]

4. Wolfe MS, Xia W, Ostaszewski BL, Diehl TS, Kimberly WT, Selkoe DJ. Two transmembrane aspartates in presenilin-1 required for presenilin endoproteolysis and gamma-secretase activity. Nature 1999;398:513–517. [PubMed: 10206644]
5. Weihofen A, Binns K, Lemberg MK, Ashman K, Martoglio B. Identification of signal peptide peptidase, a presenilin-type aspartic protease. Science 2002;296:2215–2218. [PubMed: 12077416]
6. Li YM, Xu M, Lai MT, Huang Q, Castro JL, DiMuzio-Mower J, Harrison T, Lellis C, Nadin A, Neduvelil JG, Register RB, Sardana MK, Shearman MS, Smith AL, Shi XP, Yin KC, Shafer JA, Gardell SJ. Photoactivated gamma-secretase inhibitors directed to the active site covalently label presenilin 1. Nature 2000;405:689–694. [PubMed: 10864326]
7. Urban S, Lee JR, Freeman M. Drosophila rhomboid-1 defines a family of putative intramembrane serine proteases. Cell 2001;107:173–182. [PubMed: 11672525]
8. Rawson RB. Regulated intramembrane proteolysis: from the endoplasmic reticulum to the nucleus. Essays Biochem 2002;38:155–168. [PubMed: 12463168]
9. Bier E, Jan LY, Jan YN. rhomboid, a gene required for dorsoventral axis establishment and peripheral nervous system development in Drosophila melanogaster. Genes Dev 1990;4:190–203. [PubMed: 2110920]
10. Lee JR, Urban S, Garvey CF, Freeman M. Regulated intracellular ligand transport and proteolysis control EGF signal activation in Drosophila. Cell 2001;107:161–171. [PubMed: 11672524]
11. Koonin EV, Makarova KS, Rogozin IB, Davidovic L, Letellier MC, Pellegrini L. The rhomboids: a nearly ubiquitous family of intramembrane serine proteases that probably evolved by multiple ancient horizontal gene transfers. Genome biology 2003;4:R19. [PubMed: 12620104]
12. Rather PN, Ding X, Baca-DeLancey RR, Siddiqui S. Providencia stuartii genes activated by cell-to-cell signaling and identification of a gene required for production or activity of an extracellular factor. J Bacteriol 1999;181:7185–7191. [PubMed: 10572119]
13. McQuibban GA, Saurya S, Freeman M. Mitochondrial membrane remodelling regulated by a conserved rhomboid protease. Nature 2003;423:537–541. [PubMed: 12774122]
14. Brossier F, Jewett TJ, Sibley LD, Urban S. A spatially localized rhomboid protease cleaves cell surface adhesins essential for invasion by Toxoplasma. Proc Natl Acad Sci U S A 2005;102:4146–4151. [PubMed: 15753289]
15. Cipolat S, Rudka T, Hartmann D, Costa V, Serneels L, Craessaerts K, Metzger K, Frezza C, Annaert W, D'Adamio L, Derks C, Dejaegere T, Pellegrini L, D'Hooge R, Scorrano L, De Strooper B. Mitochondrial rhomboid PARL regulates cytochrome c release during apoptosis via OPA1-dependent cristae remodeling. Cell 2006;126:163–175. [PubMed: 16839884]
16. Stevenson LG, Strisovsky K, Clemmer KM, Bhatt S, Freeman M, Rather PN. Rhomboid protease AarA mediates quorum-sensing in Providencia stuartii by activating TatA of the twin-arginine translocase. Proc Natl Acad Sci U S A 2007;104:1003–1008. [PubMed: 17215357]
17. Urban S, Wolfe MS. Reconstitution of intramembrane proteolysis in vitro reveals that pure rhomboid is sufficient for catalysis and specificity. Proc Natl Acad Sci U S A 2005;102:1883–1888. [PubMed: 15684070]
18. Lemberg MK, Menendez J, Misik A, Garcia M, Koth CM, Freeman M. Mechanism of intramembrane proteolysis investigated with purified rhomboid proteases. Embo J 2005;24:464–472. [PubMed: 15616571]
19. Wu Z, Yan N, Feng L, Oberstein A, Yan H, Baker RP, Gu L, Jeffrey PD, Urban S, Shi Y. Structural analysis of a rhomboid family intramembrane protease reveals a gating mechanism for substrate entry. Nat Struct Mol Biol 2006;13:1084–1091. [PubMed: 17099694]
20. Wang Y, Zhang Y, Ha Y. Crystal structure of a rhomboid family intramembrane protease. Nature 2006;444:179–180. [PubMed: 17051161]
21. Lemieux MJ, Fischer SJ, Cherney MM, Bateman KS, James MN. The crystal structure of the rhomboid peptidase from Haemophilus influenzae provides insight into intramembrane proteolysis. Proc Natl Acad Sci U S A 2007;104:750–754. [PubMed: 17210913]
22. Ben-Shem A, Fass D, Bibi E. Structural basis for intramembrane proteolysis by rhomboid serine proteases. Proc Natl Acad Sci U S A 2007;104:462–466. [PubMed: 17190827]

23. McCafferty DG, Lessard IA, Walsh CT. Mutational analysis of potential zinc-binding residues in the active site of the enterococcal D-Ala-D-Ala dipeptidase VanX. Biochemistry 1997;36:10498–10505. [PubMed: 9265630]
24. Butler PJ, Ubarretxena-Belandia I, Warne T, Tate CG. The Escherichia coli multidrug transporter EmrE is a dimer in the detergent-solubilised state. J Mol Biol 2004;340:797–808. [PubMed: 15223321]
25. Akiyama Y, Kanehara K, Ito K. RseP (YaeL), an Escherichia coli RIP protease, cleaves transmembrane sequences. The EMBO journal 2004;23:4434–4442. [PubMed: 15496982]
26. Fraering PCYW, Strub JM, Dolios G, LaVoie MJ, Ostaszewski BL, van Dorsselaer A, Wang R, Selkoe DJ, Wolfe MS. Purification and characterization of the human gamma-secretase complex. Biochemistry 2004;43:9774–9789. [PubMed: 15274632]
27. Urban S, Freeman M. Substrate specificity of rhomboid intramembrane proteases is governed by helix-breaking residues in the substrate transmembrane domain. Mol Cell 2003;11:1425–1434. [PubMed: 12820957]
28. Ubarretxena-Belandia I, Engelman DM. Helical membrane proteins: diversity of functions in the context of simple architecture. Current opinion in structural biology 2001;11:370–376. [PubMed: 11406389]
29. Baker RP, Young K, Feng L, Shi Y, Urban S. Enzymatic analysis of a rhomboid intramembrane protease implicates transmembrane helix 5 as the lateral substrate gate. Proc Natl Acad Sci U S A 2007;104:8257–8262. [PubMed: 17463085]
30. Okochi M, Steiner H, Fukumori A, Tanii H, Tomita T, Tanaka T, Iwatsubo T, Kudo T, Takeda M, Haass C. Presenilins mediate a dual intramembranous gamma-secretase cleavage of Notch-1. EMBO J 2002;21:5408–5416. [PubMed: 12374741]
31. Ha Y. Structural principles of intramembrane proteases. Current opinion in structural biology 2007;17:405–411. [PubMed: 17714936]
32. Urban S, Schlieper D, Freeman M. Conservation of intramembrane proteolytic activity and substrate specificity in prokaryotic and eukaryotic rhomboids. Curr Biol 2002;12:1507–1512. [PubMed: 12225666]
33. Sprang S, Standing T, Fletterick RJ, Stroud RM, Finer-Moore J, Xuong NH, Hamlin R, Rutter WJ, Craik CS. The three-dimensional structure of Asn102 mutant of trypsin: role of Asp102 in serine protease catalysis. Science 1987;237:905–909. [PubMed: 3112942]
34. Carter P, Wells JA. Dissecting the catalytic triad of a serine protease. Nature 1988;332:564–568. [PubMed: 3282170]
35. Snijder HJ, Ubarretxena-Belandia I, Blaauw M, Kalk KH, Verheij HM, Egmond MR, Dekker N, Dijkstra BW. Structural evidence for dimerization-regulated activation of an integral membrane phospholipase. Nature 1999;401:717–721. [PubMed: 10537112]
36. Kingma RL, Fragiathaki M, Snijder HJ, Dijkstra BW, Verheij HM, Dekker N, Egmond MR. Unusual catalytic triad of Escherichia coli outer membrane phospholipase A. Biochemistry 2000;39:10017–10022. [PubMed: 10955989]
37. Schroeter EH, Ilagan MX, Brunkan AL, Hecimovic S, Li YM, Xu M, Lewis HD, Saxena MT, De Strooper B, Coonrod A, Tomita T, Iwatsubo T, Moore CL, Goate A, Wolfe MS, Shearman M, Kopan R. A presenilin dimer at the core of the gamma-secretase enzyme: insights from parallel analysis of Notch 1 and APP proteolysis. Proceedings of the National Academy of Sciences of the United States of America 2003;100:13075–13080. [PubMed: 14566063]
38. Herl L, Lleo A, Thomas AV, Nyborg AC, Jansen K, Golde TE, Hyman BT, Berezovska O. Detection of presenilin-1 homodimer formation in intact cells using fluorescent lifetime imaging microscopy. Biochemical and biophysical research communications 2006;340:668–674. [PubMed: 16376853]
39. Nyborg AC, Kornilova AY, Jansen K, Ladd TB, Wolfe MS, Golde TE. Signal peptide peptidase forms a homodimer that is labeled by an active site-directed gamma-secretase inhibitor. J Biol Chem 2004;279:15153–15160. [PubMed: 14704149]
40. Nyborg AC, Herl L, Berezovska O, Thomas AV, Ladd TB, Jansen K, Hyman BT, Golde TE. Signal peptide peptidase (SPP) dimer formation as assessed by fluorescence lifetime imaging microscopy (FLIM) in intact cells. Molecular neurodegeneration 2006;1:16. [PubMed: 17105660]

41. Li YM, Lai MT, Xu M, Huang Q, DiMuzio-Mower J, Sardana MK, Shi XP, Yin KC, Shafer JA, Gardell SJ. Presenilin 1 is linked with gamma-secretase activity in the detergent solubilized state. Proceedings of the National Academy of Sciences of the United States of America 2000;97:6138–6143. [PubMed: 10801983]

42. Gu Y, Sanjo N, Chen F, Hasegawa H, Petit A, Ruan X, Li W, Shier C, Kawarai T, Schmitt-Ulms G, Westaway D, St George-Hyslop P, Fraser PE. The presenilin proteins are components of multiple membrane-bound complexes that have different biological activities. J Biol Chem 2004;279:31329–31336. [PubMed: 15123598]

43. Wang DN, Safferling M, Lemieux MJ, Griffith H, Chen Y, Li XD. Practical aspects of overexpressing bacterial secondary membrane transporters for structural studies. Biochim Biophys Acta 2003;1610:23–36. [PubMed: 12586376]

44. Chen GQ, Gouaux JE. Overexpression of bacterio-opsin in Escherichia coli as a water-soluble fusion to maltose binding protein: efficient regeneration of the fusion protein and selective cleavage with trypsin. Protein Sci 1996;5:456–467. [PubMed: 8868482]

45. Korepanova A, Moore JD, Nguyen HB, Hua Y, Cross TA, Gao F. Expression of membrane proteins from Mycobacterium tuberculosis in Escherichia coli as fusions with maltose binding protein. Protein expression and purification 2007;53:24–30. [PubMed: 17275326]

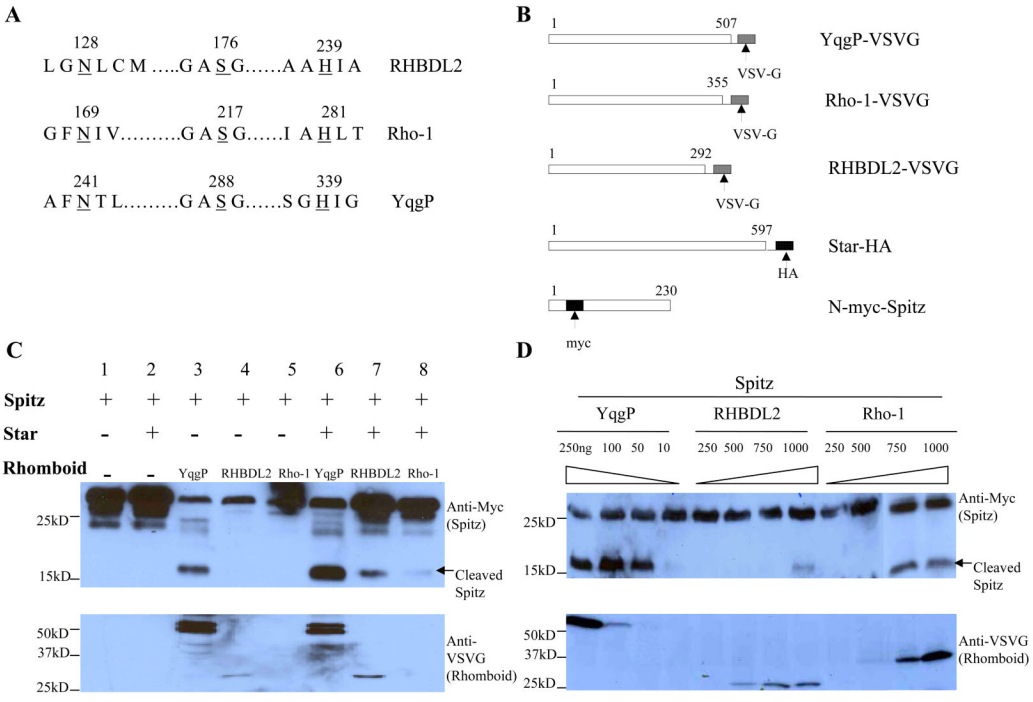

Figure 1.

High levels of Rhomboid are able to cleave Spitz independent of Star expression. (*A*) Amino acid alignment of Rhomboid sequences that contain the catalytic dyad (S-H) and a conserved Asn from different species: RHBDL2, *Homo sapiens;* Rho-1, *Drosophila*; YqgP, *Bacillus Subtilis*. The catalytic key residues are indicated by underlined amino acids. (*B*) The schematic representative of constructs that were used in the study. All Rhomboids were tagged on C-term with VSV-G. Star was tagged with HA on C-term, and a Myc tag was inserted between residue 80 and 81 of Spitz. (*C*) Spitz cleavage was Star-independent in proteolytic reconstitution in mammalian cell lines. COS-1 cells were transiently transfected with Myc-tagged Spitz, Star, and VSV-G tagged Rhomboids. *Upper panel*: full-length Spitz (26kD) and its Rhomboid cleaved form (16kD) were detected with anti-myc. *Lower panel*: overexpression levels of Rhomboids were evaluated with anti-VSV-G. (*D*) Effect of expression levels of Rhomboid on Spitz cleavage. The plasmid of pCDNA3.1-YqgP was titrated down, while those of pcDNA3.1-RHBDL2 and Rho-1 were titrated up.

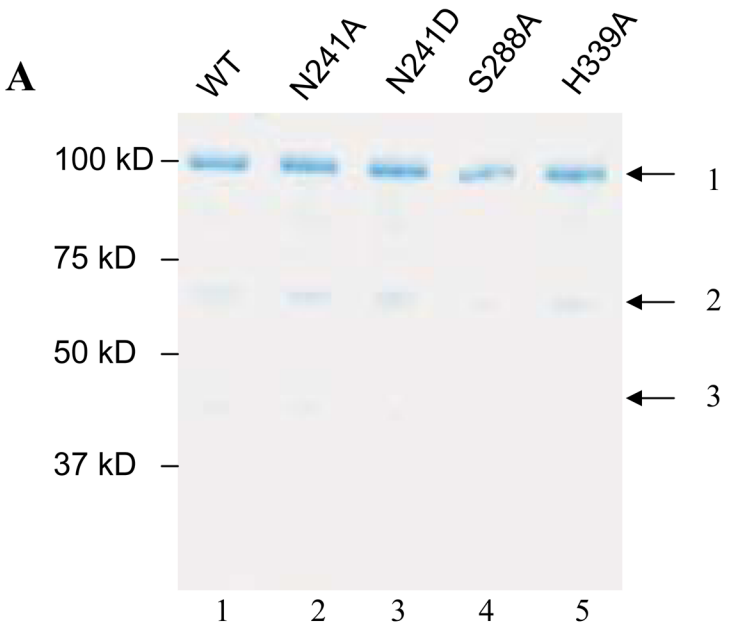

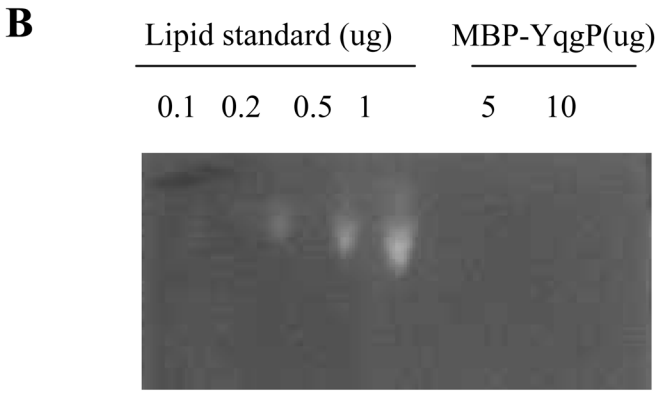

C

$Spitz_{TMD}$: (MCA)K-EKASIASGAMCALVFMLFV

TMD

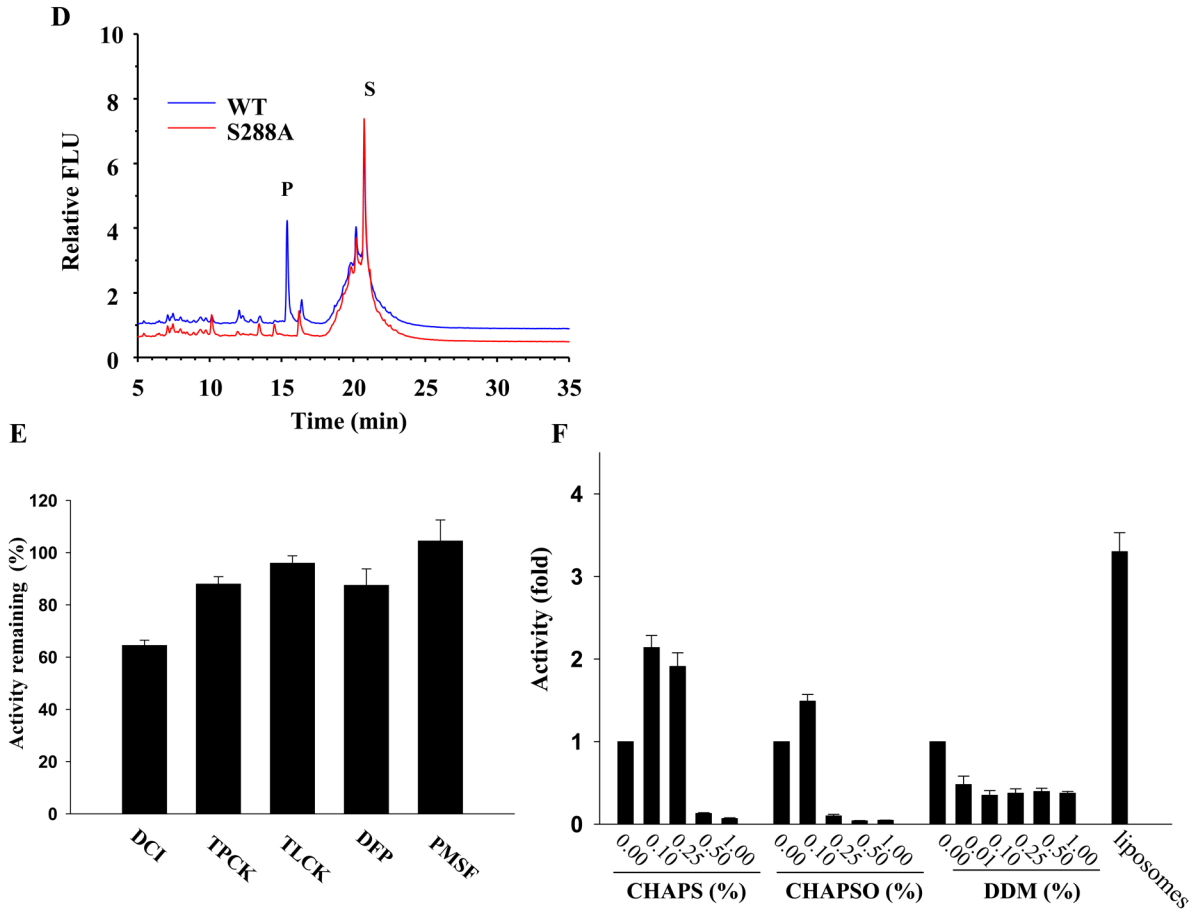

Figure 2.

In vitro reconstitution of Spitz cleavage by YqgP (*A*) Overexpression of MBP tagged YqgP and its mutants. Purified protein was analyzed on SDS-PAGE, and stained with Coomassie blue. (*B*) Lipid analysis. Lipid standard and purified MBP-YqgP were analyzed with thin-layer chromatography. (C) Fluorescence labeled peptide substrate. The peptide substrate consists of the transmembrane domain (indicated by dotted line) of Spitz and fluorescent tag MCA, which is used to monitor the cleavage of substrate. (*D*) Reconstitution of *In vitro* MBP-YqgP activity. The reaction mixture was analyzed with reverse-phase HPLC equipped with a fluorescence detector (Ex. 340 nm, Em. 405 nm). The blue line represents the cleavage activity of wild type MBP-YqgP while the red line represents the cleavage activity of the MBP-YqgP S288A (S: substrate peak; P: products peak). (*E*) Effects of commonly used serine protease inhibitors on the cleavage of $Spitz_{TMD.}$ Each inhibitor at 400 μM was used for cleavage assay (n=3, mean ± SD). (*F*) Effects of detergents and liposomes on MBP-YqgP activity. MBP-YpqP activity was assayed in the absence and the presence of detergents (CHAPS, CHAPSO, DDM or Triton X-100). There was no activity in the presence of 0.1–1% of Triton X-100. Effects of detergents on the cleavage were calculated as the percentage to the activity conducted without detergents (bar denoted with 0) (n=3, mean ± SD).

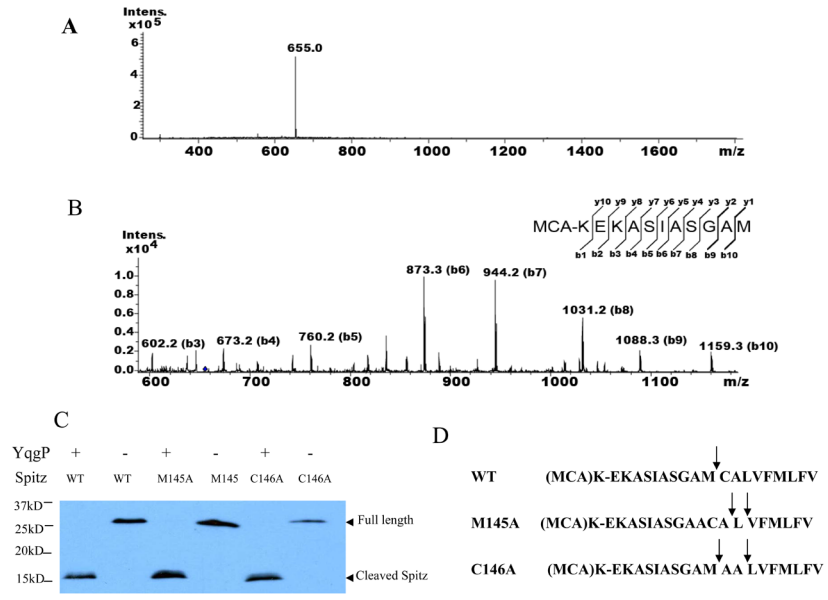

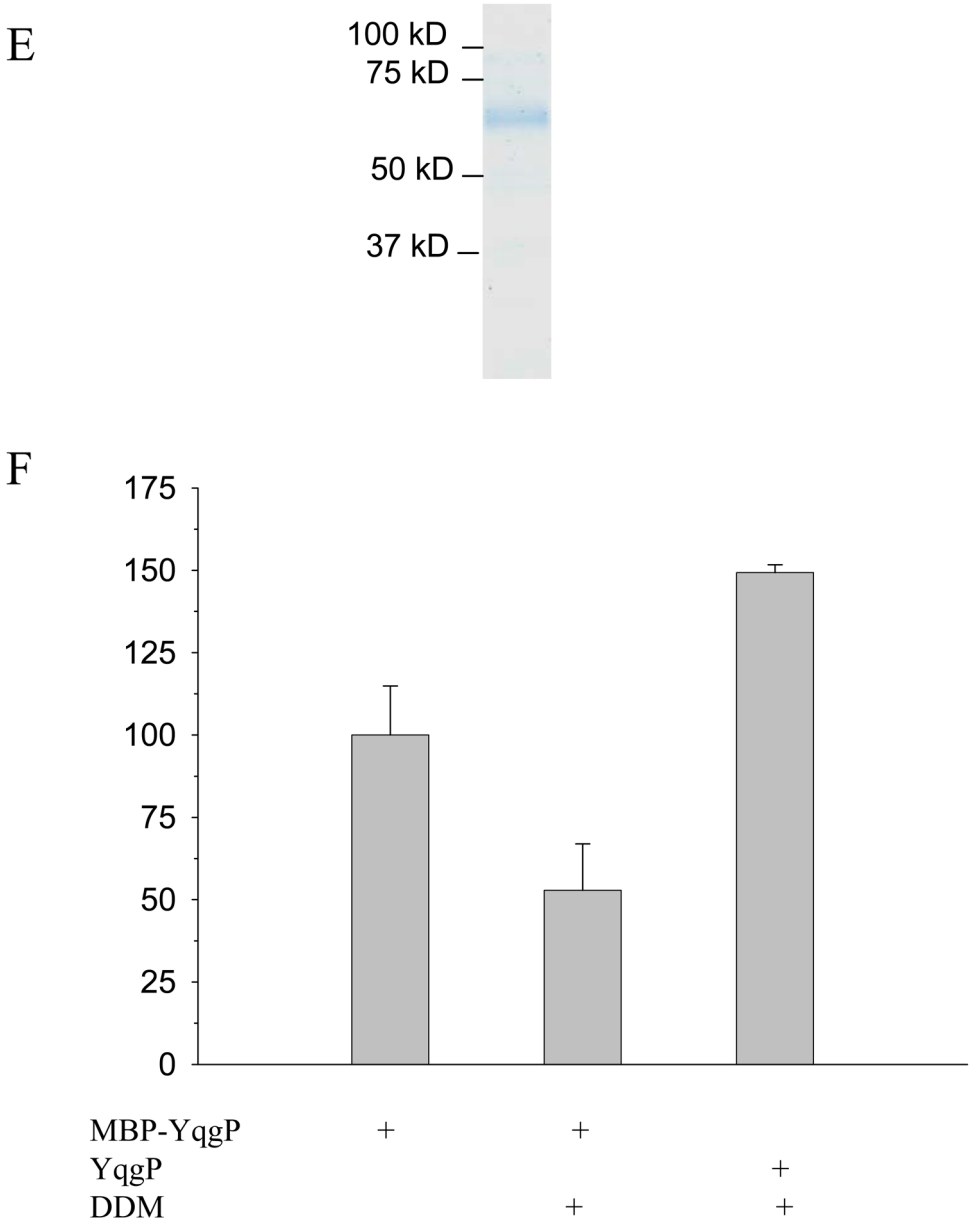

Figure 3.

Determination of $Spitz_{TMD}$ cleavage site by LC-MS/MS analysis. (*A*) The peak at 15.5 min (see Fig 2D) from reverse-phase HPLC was collected and analyzed by LC-MS/MS. A species with 655 (m/z =2) was detected. (*B*) The LC-MS/MS spectra of the 655 (m/z=2) species. Tandem MS matched a peptide with amino acid sequence to (MCA) KEKASIASGAM (b ions were denoted in the bracket). The inset scheme showed that b and y ions arise from $Spitz_{TMD}$ product. (*C*) Effects of M145A and C146A mutations on cellular YqgP activity. The Spitz WT, M145A or C146A plasmids were co-transfected into COS-1 cells with the YqgP plasmid. After 48 hrs, cell lysates were analyzed by Western analysis as described in Figure 1. (*D*) Summary of $Spitz_{TMD}$ cleavage by YqgP and the effect of mutation of Met and Cys on the cleavage. Cleavage sites were indicated by arrows. (E) Analyses of YqgP isolated from membrane fractions. Purified protein was separated by SDS-PAGE and stained with Coomassie blue. (F) Comparison of protease activity of MBP-YqgP and YqgP. The substrate

$Spitz_{TMD}$ was incubated with both forms of YqgP: MBP-YqgP isolated as a soluble protein and YqgP purified from membrane fractions. The activity was determined as described in Figure 2 (n=3 ± SD).

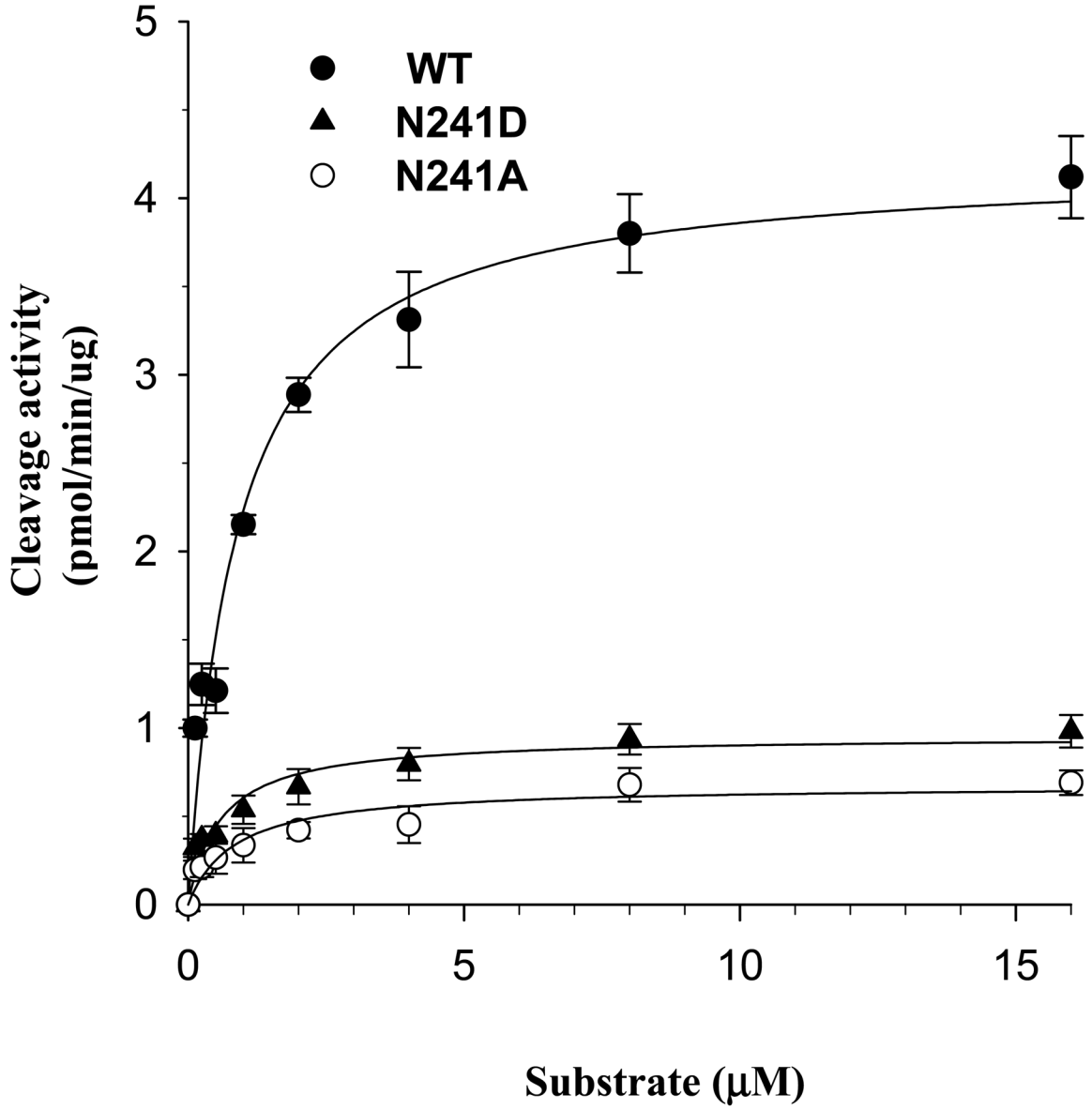

Figure 4.

Kinetic characterization of MBP-YqgP. Determination of Km and Vmax of YqgP and its mutant N241D and N241A (n=3, mean±SD). The MBP-YqgP activity was determined in the various substrate concentrations. Km and Vmax were calculated by equation: V=Vmax[S]/(Km+[S]).

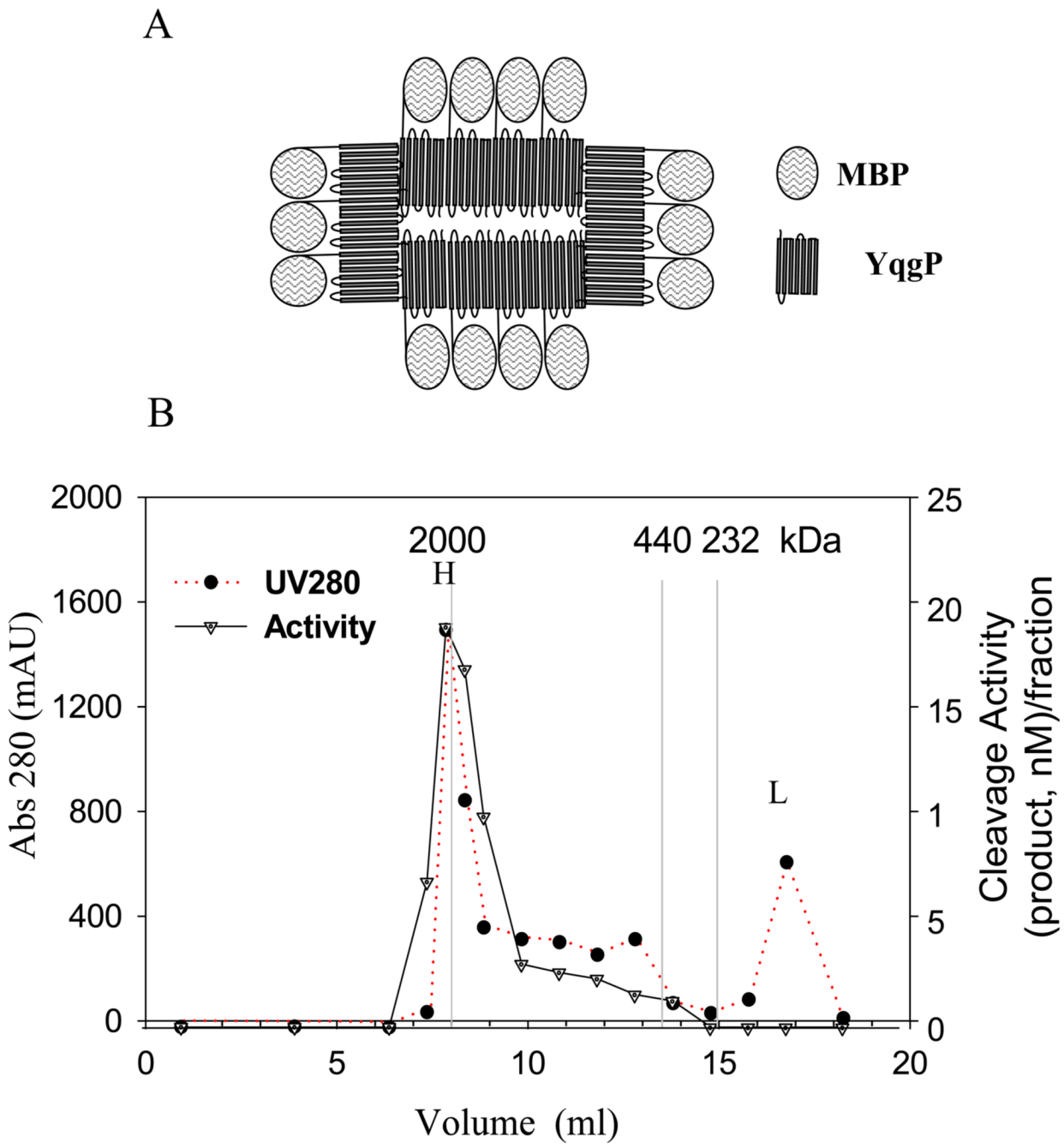

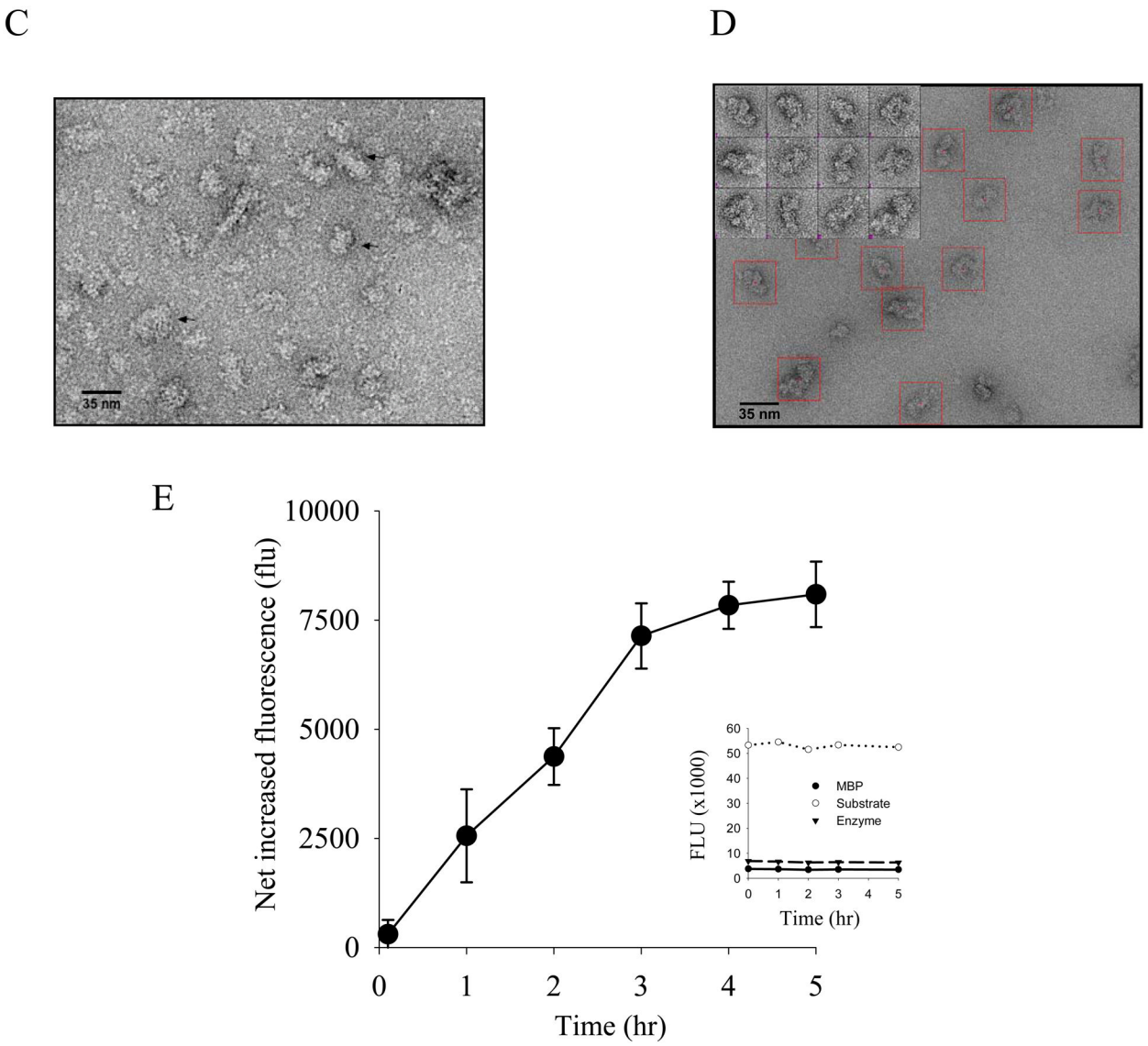

Figure 5.

MBP-YqgP exists as oligomer or multimer complexes. (*A*) Hypothetical model of mega-complex of MBP-YqgP. The hydrophilic MBP part faces outside, while the hydrophobic YqgP is buried inside. (*B*) Co-migration of MBP-YqgP protein complexes and protease activity during gel exclusion chromatography. Purified MBP-YqgP was chromatographed with Superose6 gel filtration column. The A280 profile of the eluent is shown (dotted line). Fractions were collected and assayed for MBP-YqgP activity. (*C*) Electron microscopy image of negatively stained MBP-YqgP before size exclusion chromatography and in the absence of detergent. The MBP-YqgP aggregates (marked by black arrows) are quite heterogeneous in size. (*D*)Electron microscopy image of negatively stained MBP-YqgP eluted from size exclusion chromatography (SEC) with an apparent molecular weight of 2000KDa. After SEC the MBP-YqgP aggregates are homogeneous in size with average dimensions of ~350×250Å. The insert shows individual boxed particles. The scale bars correspond to 35 nm. (E) Fluorescent changes resulted from interaction between the substrate and the MBP-YqgP complex. The MBP-YqgP-S288A or MBP (1 μM) was incubated with 8 μM of fluorescent substrate, and the fluorescent signals were monitored (Ex. 340 nm, Em. 405 nm). Substrate,

MBP or MBP-YqgP alone was used for background correction. After subtracting background, the difference (= (MBP-YqgP) – MBP) was used as index of the substrate and enzyme interaction (Y-axis). The inset scheme represents the fluorescent signal of MBP, substrate, or enzyme alone at different time points.

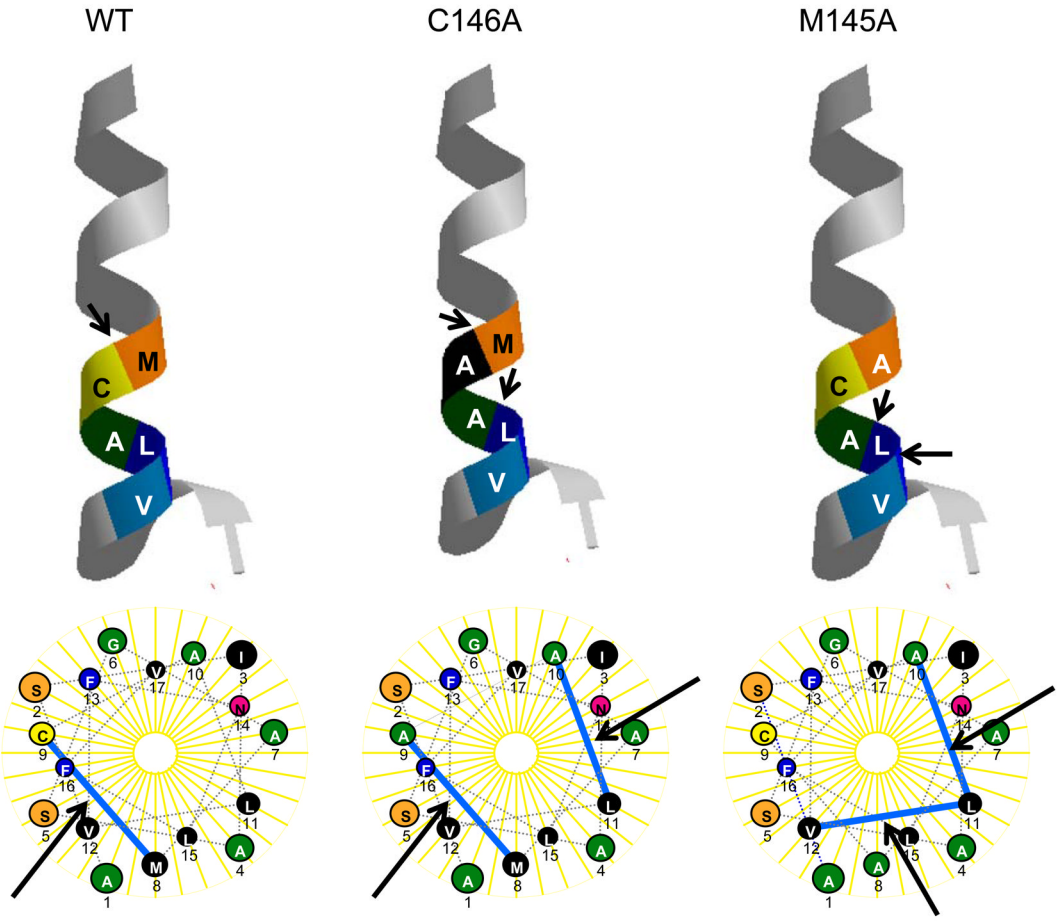

Figure 6.
Helical models of peptide substrate and cleavage sites. The helical wheel is modeled by a computer program of Lasergene 6. The cleavage sites in the WT, C146A and M145A substrates are marked by arrows.